
Graph Representations for Higher-Order Logic and Theorem Proving

Aditya Paliwal*
Google Research
adipal@google.com

Sarah Loos
Google Research
smloos@google.com

Markus Rabe
Google Research
mrabe@google.com

Kshitij Bansal
Google Research
kbsk@google.com

Christian Szegedy
Google Research
szegedy@google.com

Abstract

This paper presents the first use of graph neural networks (GNNs) for higher-order proof search and demonstrates that GNNs can improve upon state-of-the-art results in this domain. Interactive, higher-order theorem provers allow for the formalization of most mathematical theories and have been shown to pose a significant challenge for deep learning. Higher-order logic is highly expressive and, even though it is well-structured with a clearly defined grammar and semantics, there still remains no well-established method to convert formulas into graph-based representations. In this paper, we consider several graphical representations of higher-order logic and evaluate them against the HOList benchmark for higher-order theorem proving.

1 Introduction

Mathematics poses a particularly attractive learning challenge, as it can be seen as a test-bed for general-purpose reasoning. HOList (Bansal et al., 2019) is a recently published learning environment for mathematics consisting of a stateless theorem proving API, a benchmark consisting of over twenty thousand mathematical theorems and their proofs, and a neural theorem prover called DeepHOL. It builds on HOL Light (Harrison, 1996), an interactive theorem prover that has been used to formalize several mathematical theories, including much of complex analysis and the Kepler conjecture (Hales et al., 2017). The HOList environment and benchmark allows us to measure progress in automated mathematical reasoning, in particular for machine learning techniques.

The percentage of theorems that can be proven automatically by the neural theorem prover DeepHOL presented by Bansal et al. (2019) appears to be comparable with state-of-the-art algorithms in higher-order reasoning, which typically build on advanced backtracking search algorithms and proof calculi (Kaliszyk and Urban, 2014; Bentkamp et al., 2018). While these results were very promising, the reference models presented by Bansal et al. (2019) are still relatively naive—in fact we show that we can beat their best models with a bag-of-words model. The quest for model architectures that show non-trivial understanding of higher-order logic is thus wide-open.

In this paper, we explore the use of graph neural networks (GNNs) (Scarselli et al., 2009; Li et al., 2015; Gilmer et al., 2017; Wu et al., 2019). We present and compare several graph representations for higher-order logic (Section 3), and suggest a GNN architecture for processing graph representations of higher-order logic (Section 4.1).

*Google AI Resident

We focus on imitation learning, i.e. learning from human proofs. The proofs we learn from in the HOList dataset were written by human mathematicians interacting with a computer-based theorem prover. To ensure that we make meaningful progress, we evaluate all our models by measuring how many theorems they manage to prove when integrated with the DeepHOL neural theorem prover. In Section 5 we find that GNNs significantly improve the model performance, and achieve state-of-the-art performance for higher-order logic proof search by a wide margin. Our best model automatically proves 48% of the theorems in the validation set.

2 Related Work

Graph Neural Network (GNN) is an umbrella term for several kinds of neural networks that operate on graph-structured data (Wu et al., 2019; Gilmer et al., 2017; Xu et al., 2019). This family of neural networks has been successfully applied in several domains ranging from computer vision (Rapooso et al., 2017; Santoro et al., 2017), to predicting properties of molecules (Gilmer et al., 2017), to traffic prediction (Li et al., 2017). Battaglia et al. (2018) show that GNNs are capable of manipulating structured knowledge in the data and hence are a natural choice to learn meaningful representations for higher-order logic.

Similar to our work, Wang et al. (2017) apply GNNs to higher-order logic; they use graph representations of higher-order logic formulas for premise selection, resulting in a significant improvement in prediction accuracy. Our work extends their contributions by using GNNs not for premise selection, but for predicting tactics and tactic arguments. While the difference seems minor, it has a big effect on our contributions: it allows us to evaluate our models on a theorem proving benchmark where we demonstrate that our models actually prove more theorems. Because Wang et al. (2017) only predict the premises at the theorem level, they can not generate each individual proof step, and are therefore not able to use their models to generate proofs; instead they use a proxy metric that measures against existing human proofs. We are able to provide end-to-end metrics on the percentage of theorems from the validation set that can be proved using our models. This ensures that our models are learning something useful about mathematics instead of learning to exploit syntactic tricks on the data. Our findings also differ from the results of Wang et al. (2017) in a crucial aspect: we found that representations that share sub-expressions are significantly stronger than representations that use tree representations. Our graph representation allows for more sharing between expressions, as we merge variable nodes, even if they belong to different binders. Also, our representation includes all type information and has a special node for function applications, which allows us to treat variables, abstractions, and quantifiers in a uniform way.

Similar to this work, GamePad (Huang et al., 2018) and TacticToe (Gauthier et al., 2017) use imitation learning on human proofs collected from tactics-based higher-order provers (Coq and HOL4, respectively). We elected to use the HOList benchmark as opposed to the GamePad dataset due to its large corpus of human proofs readily available for training. We additionally wanted to ensure that our models performed well when used to guide proof search, which is made simple in HOList.

Traditionally, automated theorem provers were developed for first order logic, as it is easier to create complete and sound provers for it. However, most of the serious human formalization efforts (Gonthier (2008), Gonthier et al. (2013), Hales et al. (2017)) were performed using interactive proof assistants like Coq and HOL Light (Harrison (1996)), which are based on higher order logic (in which quantification over arbitrary propositions is allowed). However, the automation of higher-order theorem proving, especially at the tactic level, is a more recent research area. Deep learning has made inroads into various types of logic reasoning, for example to guide SAT solvers (Selsam and Bjørner, 2019), QBF solvers (Lederman et al., 2018), and for inductive reasoning (Dong et al., 2019).

Many authors have used TreeRNN (or TreeLSTM) architectures to encode logical statements based on their abstract syntax tree representations (Evans et al., 2018; Huang et al., 2018; Loos et al., 2017). While this seems like a natural way to encode tree-structured data, this approach greatly restricts the flow of information across the tree, especially between siblings. TreeRNNs enforce the property that a subexpression will always have the same embedding, regardless of the context in which the expression appears. While this has computational advantages, as it allows embeddings of subexpressions to be cached, it may also limit the ability of the network to effectively encode semantic information across (structurally) long distances.

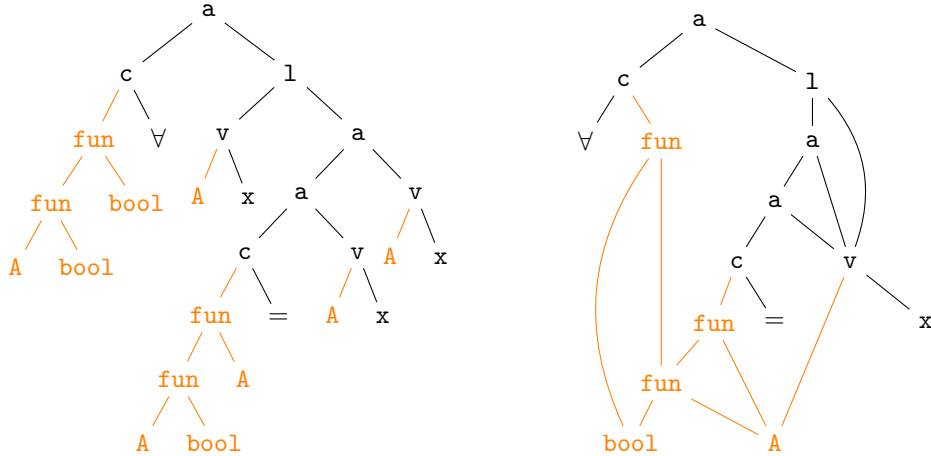


Figure 1: Comparison of two graph representations of $\forall x : x = x$. Types (e.g. `fun`, `bool`, and type variable `A`) are printed in orange. Left: abstract syntax tree representation. Right: shared sub-expressions (edge labels indicating the order of children omitted for readability). Sub-expression sharing reduces the graph size from 27 nodes to 15; the amount of sharing increases as the terms grow larger.

Conversely, Graph Neural Networks with bidirectional edges do not have a single, static embedding for each subexpression, but rather evolve embeddings for every node based on both its children and parents. Perhaps more importantly, when the graph representation allows subexpression sharing, these embeddings can draw on context from multiple occurrences. Our experimental results clearly demonstrate the importance of subexpression sharing.

3 Graph Representations of Higher-Order Logic

In this section we describe our graph representations of higher-order logic terms. The HOLLIST benchmark provides its data in the form of S-expressions. For example, the term $f(x)$, which applies a variable f to another variable x , is represented as the following string: `(a (v (fun A B) f) (v A x))`. The S-expression breaks the function application down into fundamental elements. The token `a` indicates that there is a function application, which always has two children; the function to be applied and the argument. The token `v` indicates that the function to be applied is a variable. This variable is then described as having type `fun A B` and having the name `f`. Similarly, the expression `(v A x)` describes the argument of the function application as a variable `x` with type `A`.

There are only a small number of these fundamental building blocks of HOLLIST’s S-expressions: `a` for function applications, `v` for variables, `l` for lambda expressions (also called abstractions), `c` for constants, and `fun` for function types. All other tokens are names of either variables, constants, or types, of which there are around 1200 in the dataset. Even quantifiers have no special treatment and are simply represented as functions, using the definition $(\forall) \triangleq \lambda f. (f = \lambda x. True)$.

To interpret these S-expressions with GNNs, we first parse them into one of three different graph representations:

- a shared sub-expressions graph,
- a shared sub-expressions graph with randomly added edges, or
- an abstract syntax tree with no sub-expression sharing.

In all three representations, the edges of the graph are directional (from parent to child in the abstract syntax tree); we index the edges to the children of each node from left to right.

In Figure 1 we illustrate the difference between the abstract syntax tree representation (left), and the shared sub-expressions graph (right). The variable `x` of type `A`, which originally occurred three times in the logic formula and in the abstract syntax tree, now occurs only once. It is represented by the

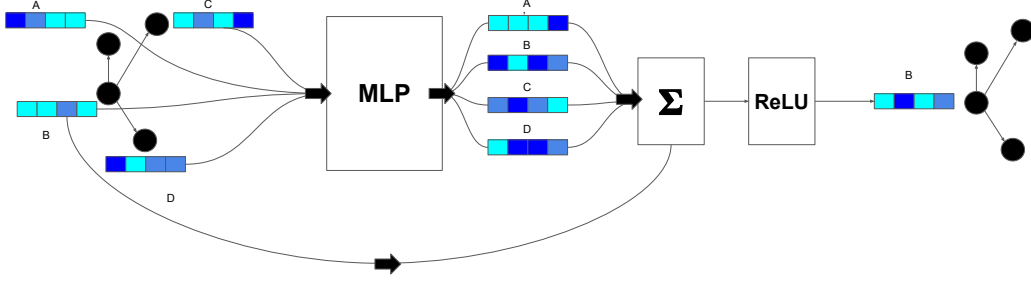


Figure 2: A single Graph Neural Network neighborhood aggregation step for node B. The features over the neighborhood are passed through an MLP, followed by a summation and a non-linearity. The output that follows is the hidden feature for node B for the next step.

S-expression ($v \ x \ A$), and the root node of this expression now has three parents that keep track of the locations of each of its original occurrences. Note that sub-expression sharing also happens over types. In this example, variable x has type A, so every other expression with type or sub-type A is now connected through this node.

We further consider the addition of random edges in the graph representation. We add 3 outgoing edges per node to random targets, and label these edges to make them distinguishable from regular edges in the graph. This approximates the construction of expander graphs and therefore provides excellent connectivity properties of the resulting graph with little overhead.

4 Model Architecture

In this section we provide the details of our neural network architecture, starting with basics of message-passing GNNs in Section 4.1, which we use for embedding statements in higher-order logic. We then detail the prediction tasks necessary for guiding proof search and our imitation learning approach, which trains on human proofs, in Section 4.2.

4.1 Graph Neural Networks

Graph Neural Networks compute embeddings for nodes in a graph via consecutive rounds of end-to-end differentiable message passing. The input to a Graph Neural Network is a graph $G = (V, E)$ where V is the set of nodes and E is the set of (directed) edges. For the graph representations of higher-order logic presented in Section 3, we represent each bi-directional edge as two edges. Each node $v \in V$ is associated with a feature vector x_v and each edge in the graph $e \in E$ is associated with a feature vector x_e . The Graph Neural Network computes node embeddings h_v for each node $v \in V$ via an iterative message passing process of T rounds:

1. Embed the node and edge features, x_v and x_e into high dimensional space using MLPs:

$$h_v^1 = \text{MLP}_V(x_v)$$

$$h_e = \text{MLP}_E(x_e)$$

2. For each round $t \in \{2, \dots, T\}$, and for each edge $(u, v) = e \in E$, pass the node embeddings from the previous step h_u^{t-1} and h_v^{t-1} and the edge embedding h_e into an MLP to generate messages:

$$s_{u,v}^t = \text{MLP}_{\text{edge}}([h_u^{t-1}, h_v^{t-1}, h_e])$$

$$\hat{s}_{u,v}^t = \hat{\text{MLP}}_{\text{edge}}([h_v^{t-1}, h_u^{t-1}, h_e])$$

3. For each node $v \in V$, sum over the messages sent and received by this node, over its neighbors $N(v)$ and pass them through an MLP to aggregate them:

$$h_v^t = h_v^{t-1} + \text{MLP}_{\text{aggr}} \left(\left[h_v^{t-1}, \sum_{u \in N(v)} s_{v,u}^t, \sum_{u \in N(v)} \hat{s}_{v,u}^t \right] \right)$$

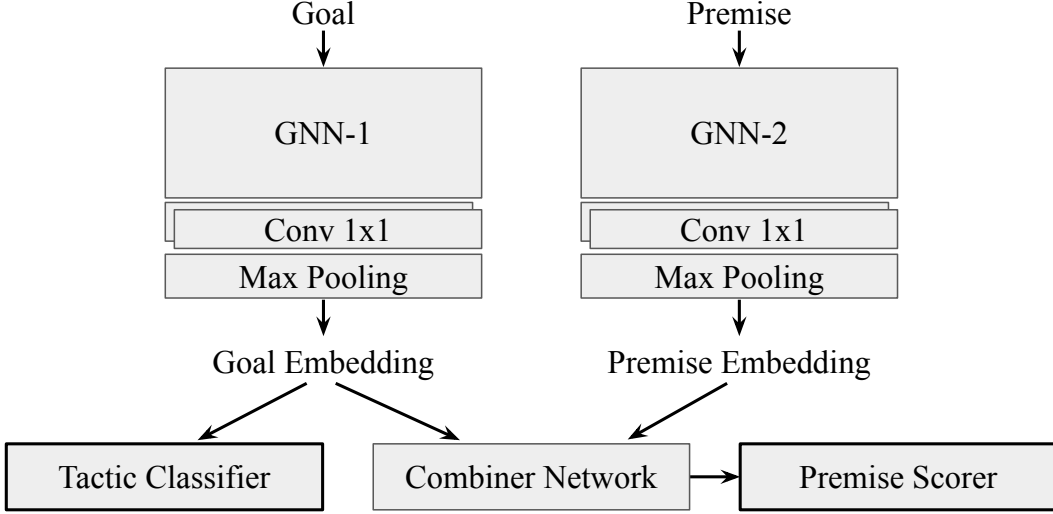


Figure 3: Diagram of the model architecture. At every step of the proof, the current goal is embedded using GNN-1. Based on the goal embedding, the model predicts the next tactic to apply from a fixed set of 41 tactics. The goal embeddings are also used to score every preceding theorem, called premises. Premises are also embedded using a graph neural network (GNN-2). Higher scores indicate the given premise is predicted to be useful for proving the current goal. Full details presented in Section 4.2.

MLP_V , MLP_E , MLP_{edge} , $\hat{\text{MLP}}_{\text{edge}}$ and MLP_{aggr} are multi-layer perceptrons, $[\cdot, \cdot]$ is the vector concatenation operator, and h_v^t represents the embedding of node v after t rounds of message passing. A multi-layer perceptron (MLP), is a function $\text{MLP} : \mathbb{R}^a \rightarrow \mathbb{R}^b$, that maps vectors in the input space to the output space via successive applications of linear transformations and non-linear activations.

The final set of node embeddings returned by the Graph Neural Network is given by $h_v = h_v^T$ where T is the number of message passing rounds. These node embeddings represent information from the T -hop neighborhood of each node in the graph. A single step of message passing over a single node of a graph is shown in Figure 2.

4.2 Complete Model Architecture

The full architecture is depicted in Figure 3. The network takes the current goal (an intermediate state in a proof search) and a candidate premise.

It then generates node embeddings $G(g)$ and $P(p)$ for the graph representations of both the goal g and premise p using identical GNNs; GNN-1 and GNN-2 do not share weights. To make the architecture computationally tractable, the depth of each node embedding is relatively small (128). We do two 1x1 convolutions to expand the depth (to 512 and then to 1,024) immediately before max pooling, resulting in a goal embedding and premise embedding, each of size 1,024.

The tactic classifier selects from a fixed set of 41 tactics. It uses two fully connected layers, followed by a linear layer to produce logits for a softmax tactic classifier. The combiner network concatenates the goal and premise embeddings, as well as their element-wise multiplication, followed by three fully connected layers. The model uses sigmoid cross-entropy to score how useful an individual premise is for the given goal. It was important to apply dropout throughout the network.

This architecture was trained on the proofs written by humans and released in the HOList dataset. For evaluation, we plug the models into the breadth-first proof search provided by the the HOList environment. We first start with the top level goal which is the top level theorem to be proved. To process a goal (or "subgoals" for newly created goals), we apply one of the 41 tactics that may take a

list of already proven theorems as parameters.² Once a goal is set to be processed, we pick the top- k_1 highest scoring tactics from the softmax tactic classifier (see Figure 3). Then the combiner network is evaluated for to each (g, p_i) pairs of the current goal g and possible tactic parameter p_i (which are all the definitions and theorems preceding the top level goal in the theorem database). Note that this computation is accelerated significantly by pre-computing the premise-embeddings $P(p_i)$, and therefore only the combiner network has to be evaluated for each pair of embeddings $G(g), P(p_i)$, where $G(g)$ denotes the goal embedding of the currently processed goal. In total, there are 19,262 theorems and definitions in the theorem database. Only the top- k_2 highest scoring premises are chosen as tactic arguments. In our setting, we used $k_1 = 5, k_2 = 20$.

A tactic application might fail or may be successful. Failed applications are logged, but ignored for proof search. If the tactic application is successful, it might close (that is: prove) the goal or generate a new list of subgoals (or proof obligations). The original goal is closed if each of its subgoals are closed. During proof search, the HOList proof-search graph maintains several alternative branches of subgoals to be closed. Proof search stops if the top-level goal closes, that is if any of the alternative branches closes.

Note that in contrast to earlier premise selection works, we generate new tactic parameter lists for each subgoal during proof-search, not just a single list of premises for the top-level goal.

5 Experiments

Here we present our experimental results, including details about the HOList benchmark, which we used for training. Our main metric is the number of proofs found for theorems in the validation set by each model. We additionally provide an in-depth analysis of the model performance and of the proofs found by our GNN models.

5.1 The HOList Benchmark and Dataset

We test our models on the HOList (Bansal et al., 2019) benchmark, which is based on the complex analysis corpus of HOL Light (Harrison, 1996). The training set is derived from the proofs of 10,200 top-level theorems and has around 375,000 proof steps (subgoals) to learn from. We have evaluated the end-to-end prover performance on the standard validation split of HOList which consists of 3,225 held out theorems of the complex analysis corpus.

In total, there are 19,262 theorems and definitions in the HOList corpus. These theorems are proved in a sequential order, so for any given goal, all theorems and definitions that precede it in the corpus are eligible premises. However, only the top 20 premises (ranked according to the premise scorer) are selected for each tactic application.

5.2 Evaluation Metrics

The primary way that we evaluate our models is by hooking them up to the HOL Light theorem prover, using them to guide the proof search, and then counting how many theorems they can prove. However, it takes several hours to run the prover on the validation set, even in a distributed manner. If we were to use this metric during training, it would slow down training of our models by several orders of magnitude, so we instead train using two proxy metrics:

- We look at the accuracy of the tactic prediction output, which decides which one of the 41 possible tactics is to be applied for a given goal. It is often the case that more than one choice of tactic would work, but to determine if a tactic is correct, we would need to try it in the prover. Instead, for the proxy metric, we only count a tactic correct if it was the exact tactic applied in the human proof, as our data contains only a single proof per theorem.
- We monitor the relative prediction accuracy for the tactic parameter selection, which is the ratio of cases in which a true tactic parameter is scored higher than some randomly sampled parameter. Again, there is often more than one “true parameter”, but we only consider the set of premises that were used as tactic parameters in the human proof.

²The interpretation of the tactic parameters depends on the type of the tactic. For MESON_TAC these are premises that the tactic can use for proving the statement in HOL Light’s built-in first order reasoning algorithm. For REWRITE_TAC, these should be equations that should be applied for rewriting the goal statement.

Table 1: Number of proofs closed by different models with different graph representations, compared against previous state of the art and bag of words model as baselines.

Representation	Network Architecture	% Proofs Closed (Validation Set)
Baseline: S-expression as a string	WaveNet (Bansal et al., 2019)	32.65%
Baseline: Bag of words	Max pooling only	37.98%
Shared sub-expression graph	0 hops	41.79%
Shared sub-expression graph	2 hops	46.20%
Shared sub-expression graph	4 hops	48.06%
Abstract Syntax Tree	0 hops	37.82%
Abstract Syntax Tree	2 hops	43.44%
Abstract Syntax Tree	4 hops	45.33%
Sharing + Random Edges	0 hops	40.99%
Sharing + Random Edges	2 hops	47.25%
Sharing + Random Edges	4 hops	47.68%

We then perform the computationally expensive evaluation only on the best checkpoint (according to the proxy metrics): running the prover once over the validation set using the parameterized tactics predicted by the checkpoint to guide proof search. This *percentage of proofs closed* in the validation set is the primary metric that we use to establish the proving power of a given checkpoint. It evaluates whether a trained model is effective at automatically proving newly encountered theorems.

5.3 Results

We train several models using the architecture described in Section 4.2, varying the number of message passing rounds in the GNN and the representation of the higher-order logic formulas as graphs as described in Section 3.

We present the results of our models, along with our baselines in Table 1. Our 4-hops shared sub-expression graph network achieves the state-of-the-art result on the HOList benchmark, closing 48.06% of the proofs. This is a major step up from the baseline models in the HOList paper (32.65%) and even outperforms the reported 38.9% of their tactic-dependent loop model, which was trained using a combination of reinforcement learning and imitation learning. We also observe that a simple bag-of-words model with large word embedding sizes also manages to close 37.98% of all proofs. The GNN models with 0 message passing steps are roughly equivalent to the bag of words max pooling model, except that there is significant deduplication in the two shared sub-expression graphs and the 0-hop models also have additional MLPs between the word embedding lookup step and the max pooling step.

With respect to graph representations, we note that every single model that uses the graph neural network with a non-zero number of message passing steps beats all other baselines.

5.4 Analysis

In Table 1 we can see that the number of proofs closed by the model increases with additional hops (message passing steps), regardless of the graph representation used. This indicates that additional information about the structure of higher-order logic formulas provides the model with the capacity to learn better embeddings.

The graph representation with random edges considerably improves the performance of the 2 hop network, but not the 4 hop network. This suggests that the addition of random edges increases the field-of-view into the graph for the networks, but the benefits diminish after some point.

Similar to (Bansal et al., 2019), we also study the total number proofs closed by the union of all the models trained. In Table 2, we can see that the union of all models trained on a given representation can close $\sim 6\%$ more proofs than the best individual model. The union of the theorems proven by at least one of our GNN models is 57.95%, which is almost 10% higher than the best individual model. This indicates that there is still some variation in what the different GNN models learn and that there is room for improvement.

Table 2: Union of proofs closed in each representation.

Graph Representation	% Proofs Closed
Shared sub-expression graph	53.82%
Abstract Syntax Tree	51.41%
Sharing + Random Edges	53.73%
Total	57.95%

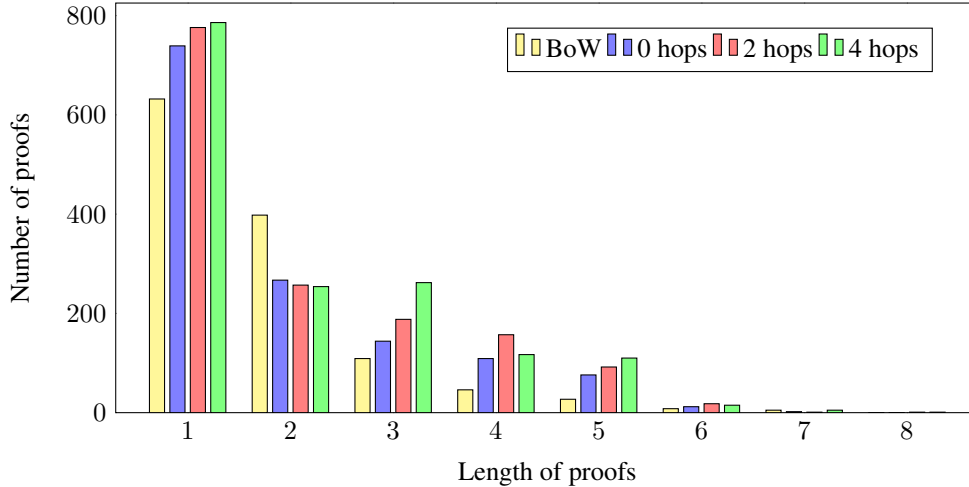


Figure 4: A comparison of the length of proofs found by the bag-of-words model (BoW) and the Shared sub-expression graph models with different numbers of hops.

We observed that GNN models with four hops not only find more proofs, but also finds longer proofs on average (2.1 steps vs 1.9 on average) than with zero hops. The distribution of proof lengths is presented in Figure 4. Comparing the proofs found by the 4 hops model to those found by the 0 hops model reveals that 167 of the 201 additional proofs found are of length 3 and higher.

We provide additional analysis in Appendix A.2.

6 Conclusions and Future Work

We present the first use of graph neural networks to guide higher-order theorem proving. We experiment with a few canonical ways of representing higher-order logic expressions as graphs and demonstrate that graph neural networks can significantly improve over non-structured representations, especially when the structure of the graph allows for sharing of sub-expressions. Using GNNs, we are able to significantly improve previous state-of-the-art results for imitation learning on the HOList theorem set and proof search environment.

We observed that increasing the number of message passing steps resulted in improved accuracy on the training and evaluation sets, and also led to a larger percentage of closed proofs. While the number of message passing steps in our experiments was limited, we believe that adding more hops will improve the neural network’s ability to capture additional structural information from higher-order logic expressions. In future work, we hope to scale these networks and test this hypothesis thoroughly.

In the experiments presented in this paper, we predict tactics and their arguments by looking only at the conclusion of the current sub-goal and ignoring any local assumptions that could be crucial to the proof. This is a serious limitation for our system, and in future work we would like to include the local assumptions list when generating the embedding of the goal. We expect this to be a natural extension for GNNs, which can easily extend graph representations to include additional expressions.

References

- Kshitij Bansal, Sarah M Loos, Markus N Rabe, Christian Szegedy, and Stewart Wilcox. 2019. HOList: An Environment for Machine Learning of Higher-Order Theorem Proving. *ICML 2019. International Conference on Machine Learning* (2019).
- Peter W. Battaglia, Jessica B. Hamrick, Victor Bapst, Alvaro Sanchez-Gonzalez, Vinícius Flores Zambaldi, Mateusz Malinowski, Andrea Tacchetti, David Raposo, Adam Santoro, Ryan Faulkner, Çağlar Gülçehre, Francis Song, Andrew J. Ballard, Justin Gilmer, George E. Dahl, Ashish Vaswani, Kelsey Allen, Charles Nash, Victoria Langston, Chris Dyer, Nicolas Heess, Daan Wierstra, Pushmeet Kohli, Matthew Botvinick, Oriol Vinyals, Yujia Li, and Razvan Pascanu. 2018. Relational inductive biases, deep learning, and graph networks. *CoRR* abs/1806.01261 (2018). arXiv:1806.01261 <http://arxiv.org/abs/1806.01261>
- Alexander Bentkamp, Jasmin Christian Blanchette, Simon Cruanes, and Uwe Waldmann. 2018. Superposition for Lambda-Free Higher-Order Logic. In *Automated Reasoning*, Didier Galmiche, Stephan Schulz, and Roberto Sebastiani (Eds.). Springer International Publishing, Cham, 28–46.
- Christopher Burges, Tal Shaked, Erin Renshaw, Ari Lazier, Matt Deeds, Nicole Hamilton, and Gregory N Hullender. 2005. Learning to rank using gradient descent. In *Proceedings of the 22nd International Conference on Machine Learning (ICML-05)*. 89–96.
- Honghua Dong, Jiayuan Mao, Tian Lin, Chong Wang, Lihong Li, and Denny Zhou. 2019. Neural Logic Machines. *ICLR 2019. International Conference on Learning Representations* (2019).
- Elad ET Eban, Mariano Schain, Alan Mackey, Ariel Gordon, Rif A Saurous, and Gal Elidan. 2017. Scalable learning of non-decomposable objectives. *Proceedings of the 20th International Conference on Artificial Intelligence and Statistics (AISTATS)* (2017).
- Richard Evans, David Saxton, David Amos, Pushmeet Kohli, and Edward Grefenstette. 2018. Can Neural Networks Understand Logical Entailment? *ICLR 2018. International Conference on Learning Representations* (2018).
- Thibault Gauthier, Cezary Kaliszyk, and Josef Urban. 2017. TacticToe: Learning to reason with HOL4 Tactics. In *LPAR-21. 21st International Conference on Logic for Programming, Artificial Intelligence and Reasoning*, Vol. 46. 125–143.
- Justin Gilmer, Samuel S. Schoenholz, Patrick F. Riley, Oriol Vinyals, and George E. Dahl. 2017. Neural Message Passing for Quantum Chemistry. *CoRR* abs/1704.01212 (2017). arXiv:1704.01212 <http://arxiv.org/abs/1704.01212>
- Georges Gonthier. 2008. Formal proof—the four-color theorem. *Notices of the AMS* 55, 11 (2008), 1382–1393.
- Georges Gonthier, Andrea Asperti, Jeremy Avigad, Yves Bertot, Cyril Cohen, François Garillot, Stéphane Le Roux, Assia Mahboubi, Russell O’Connor, Sidi Ould Biha, Ioana Pasca, Laurence Rideau, Alexey Solovyev, Enrico Tassi, and Laurent Théry. 2013. A Machine-Checked Proof of the Odd Order Theorem. In *ITP*. 163–179.
- Thomas Hales, Mark Adams, Gertrud Bauer, Tat Dat Dang, John Harrison, Hoang Le Truong, Cezary Kaliszyk, Victor Magron, Sean McLaughlin, Tat Thang Nguyen, et al. 2017. A formal proof of the Kepler conjecture. In *Forum of Mathematics, Pi*, Vol. 5. Cambridge University Press.
- John Harrison. 1996. HOL Light: A Tutorial Introduction. In *FMCAD*. 265–269.
- Daniel Huang, Prafulla Dhariwal, Dawn Song, and Ilya Sutskever. 2018. GamePad: A Learning Environment for Theorem Proving. *ICLR 2018. International Conference on Learning Representations* (2018).
- Cezary Kaliszyk and Josef Urban. 2014. Learning-assisted automated reasoning with Flyspeck. *Journal of Automated Reasoning* 53, 2 (2014), 173–213.
- Diederik P Kingma and Jimmy Ba. 2014. Adam: A method for stochastic optimization. *arXiv preprint arXiv:1412.6980* (2014).

- Gil Lederman, Markus N. Rabe, and Sanjit A. Seshia. 2018. Learning Heuristics for Automated Reasoning through Deep Reinforcement Learning. *CoRR* abs/1807.08058 (2018). arXiv:1807.08058 <http://arxiv.org/abs/1807.08058>
- Yujia Li, Daniel Tarlow, Marc Brockschmidt, and Richard Zemel. 2015. Gated graph sequence neural networks. *arXiv preprint arXiv:1511.05493* (2015).
- Yaguang Li, Rose Yu, Cyrus Shahabi, and Yan Liu. 2017. Graph Convolutional Recurrent Neural Network: Data-Driven Traffic Forecasting. *CoRR* abs/1707.01926 (2017). arXiv:1707.01926 <http://arxiv.org/abs/1707.01926>
- Sarah Loos, Geoffrey Irving, Christian Szegedy, and Cezary Kaliszyk. 2017. Deep network guided proof search. *LPAR-21. 21st International Conference on Logic for Programming, Artificial Intelligence and Reasoning* (2017).
- Boris Teodorovich Polyak. 1990. A new method of stochastic approximation type. *Avtomatika i telemekhanika* 7 (1990), 98–107.
- Boris T Polyak and Anatoli B Juditsky. 1992. Acceleration of stochastic approximation by averaging. *SIAM Journal on Control and Optimization* 30, 4 (1992), 838–855.
- David Raposo, Adam Santoro, David G. T. Barrett, Razvan Pascanu, Timothy P. Lillicrap, and Peter W. Battaglia. 2017. Discovering objects and their relations from entangled scene representations. *CoRR* abs/1702.05068 (2017). arXiv:1702.05068 <http://arxiv.org/abs/1702.05068>
- Adam Santoro, David Raposo, David G. T. Barrett, Mateusz Malinowski, Razvan Pascanu, Peter Battaglia, and Timothy P. Lillicrap. 2017. A simple neural network module for relational reasoning. *CoRR* abs/1706.01427 (2017). arXiv:1706.01427 <http://arxiv.org/abs/1706.01427>
- Franco Scarselli, Marco Gori, Ah Chung Tsoi, Markus Hagenbuchner, and Gabriele Monfardini. 2009. The graph neural network model. *IEEE Transactions on Neural Networks* 20, 1 (2009), 61–80.
- Daniel Selsam and Nikolaj Bjørner. 2019. Guiding High-Performance SAT Solvers with Unsat-Core Predictions. *SAT 2019, The 22nd International Conference on Theory and Applications of Satisfiability Testing* (2019).
- Mingzhe Wang, Yihe Tang, Jian Wang, and Jia Deng. 2017. Premise selection for theorem proving by deep graph embedding. In *Advances in Neural Information Processing Systems*. 2786–2796.
- Zonghan Wu, Shirui Pan, Fengwen Chen, Guodong Long, Chengqi Zhang, and Philip S. Yu. 2019. A Comprehensive Survey on Graph Neural Networks. *CoRR* abs/1901.00596 (2019). arXiv:1901.00596 <http://arxiv.org/abs/1901.00596>
- Keyulu Xu, Weihua Hu, Jure Leskovec, and Stefanie Jegelka. 2019. How Powerful are Graph Neural Networks? *ICLR 2019. International Conference on Learning Representations* (2019).

A Appendix

A.1 Hyperparameters and Implementation Details

In this section, we give a complete description of our implementation and hardware setup, including hyper-parameter settings and a more detailed description of the losses we used. These hyper-parameters did not vary between experiments presented in the paper, and are presented here solely to aid reproducibility of the best-performing result.

Choosing Negative Examples. For each theorem in the HOList training set, there is only one human proof. We generate positive training examples from each step of the human proof with three values: the goal that is being proved at that step, the tactic applied to it, and a list of theorem parameters passed to the tactic (or a special token if no parameters were used). To generate positive (goal, premise) pairs, we sample a premise from this list of theorem parameters. In each batch, we sample 16 positive (goal, premise) pairs from our training data.

Because we only have successful human proofs, we select our negative training examples by sampling uniformly from the set of all theorems that were used at least once as positive training examples. Every goal in the batch is then paired with 15 randomly sampled theorems and labeled as negative examples (adding $15 \times 16 = 240$ negative examples to the batch).

Since the combiner network is quite small relative to the GNN embedding networks, we reuse all 256 embedded premises (positive and negative) as negative premise examples for the remaining goals in the batch (adding $15 \times 256 = 3,840$ negative examples to the batch), giving a total batch size of 4,096.

Loss Functions. In addition to the cross-entropy loss for both tactics and pairwise scores as described in the paper, we also use the AUCROC loss (Burges et al., 2005; Eban et al., 2017) to directly relate positive and negative premise examples within a batch. The AUCROC loss minimizes the area under the ROC curve and is implemented as follows.

$$AUCROC_b = \sum_i \sum_j loss(logit_i - logit_j)$$
$$loss(l) = \ln(1 + e^{-l})$$

Where i ranges over the positive premises in batch b and j ranges over the negatives in b . Because our final prediction task will be to rank premises for just one given goal, we double the loss for logits that compare positive and negative premises for the same goal.

For the total loss, we take a weighted sum of the cross-entropy loss on the tactic classifier (weight = 1.0), the cross-entropy loss on the pairwise scorer (weight = 0.2), and the AUCROC loss (weight = 4.0).

Optimizers, Learning Rate, Dropout, and Polyak Averaging. For training, we use an Adam Optimizer (Kingma and Ba, 2014) with initial learning rate 0.0001 and decay rate 0.98. Excluding the two GNNs, dropout is added before every dense layer of the network with a “keep probability” of 0.7. For our evaluation checkpoints, we also use moving exponential parameter averaging with rate 0.9999 per step (Polyak, 1990; Polyak and Juditsky, 1992).

GNN Hyperparameters.

- **Graph Neural Network**
 - The graph neural network begins by projecting the raw node features x_v and raw edge features x_e to vectors of size 128 using an MLP with two hidden layers of sizes 256 and 128 with ReLU activations (MLP_V and MLP_E). The resulting embeddings are denoted by h_v^1 and x_e .
 - We then perform t rounds of message passing as per the equations shown in 4.1. MLP_{edge} , \hat{MLP}_{edge} and MLP_{aggr} have an identical configuration with two layers, with hidden sizes 256 and 128 and ReLU activations. The MLPs don’t share weights across message passing steps.
 - The final node embedding has size 128.

- A dropout of 0.5 is applied to all MLPs.
- **Graph Aggregator**
 - The node embeddings h_v returned by the Graph Neural Network are aggregated into a single vector that represents the embedding of the entire graph.
 - Using two Conv 1 x 1 layers, we expand the 128 dimensional node embeddings to 512, and then 1024, with ReLU activations and a dropout rate of 0.5. Then we perform max pooling over all node embeddings to create a single vector of size 1024.

Hardware. We used eight NVIDIA Tesla V100 GPUs for distributed training, an additional GPU was used purely for evaluation, and we maintained a separate parameter server on a CPU machine.

A.2 Additional Analysis

In Table 3, we count, for each graph representation, the number of proofs closed by a model that none of the other 2 models closed. We observe that GNNs with more hops consistently close more distinct proofs, indicating that they learn better embeddings. We also measure the average token-length of the subgoals in the proofs closed by each of the models. We observe that for the Abstract Syntax Tree representation and the representation with random edges, GNNs with more hops have longer subgoals. However, this does not hold true for the models trained with the Shared sub-expression graph representation.

In Figure 5 we compare the distribution of tactic applications of our best GNN model versus the model in the HOList benchmark (Bansal et al., 2019) and the max-pooling-only network. We note that the HOList model has a strong preference for REWRITE_TAC, SIMP_TAC and AMS_MESON_TAC relative to the GNN and max-pooling-only networks. On the other hand, the GNN model has a strong preference for PURE_ONCE_REWRITE_TAC relative to the other models. Apart from these, the differences between the max-pooling-only network and the best GNN model are subtle, and their effect on the prover is non-trivial to analyse.

Table 3: Number of proofs closed by model but not any other model, using given representation.

Graph Representation	Network Architecture	% Proofs Closed Uniquely (Validation Set)	Avg length of subgoals
Shared sub-expression graph	0 hops	1.39%	1456.00
Shared sub-expression graph	2 hops	2.26%	1486.61
Shared sub-expression graph	4 hops	3.59%	1419.35
Abstract Syntax Tree	0 hops	1.51%	1285.98
Abstract Syntax Tree	2 hops	2.57%	1418.15
Abstract Syntax Tree	4 hops	4.00%	1452.24
Sharing + Random Edges	0 hops	1.30%	1348.08
Sharing + Random Edges	2 hops	2.69%	1416.44
Sharing + Random Edges	4 hops	2.97%	1422.73

In Table 4, we can see that the union of proofs closed by the ensemble of the best GNN model and the two baseline models is 52.31%. This is smaller than the ensemble of the three GNN models using the shared sub-expression graph representation (53.82%). This indicates that varying the number of message passing iterations in the GNN can alone give a richer ensemble than by using three different neural network architectures (GNN, Bag of words and WaveNet). The bulk of the unique proofs, come from the GNN model and it is also the smallest among the three models.

Table 4: Union of proofs closed and proofs closed uniquely for best model and baselines.

Model	% Proofs Closed	% Proofs Closed Uniquely	# Model Params
Our best model	48.06%	8.77%	21M
HOList model	32.65%	2.10%	47M
Max pooling only model	37.98%	0.62%	34M
Total	52.31%	-	-

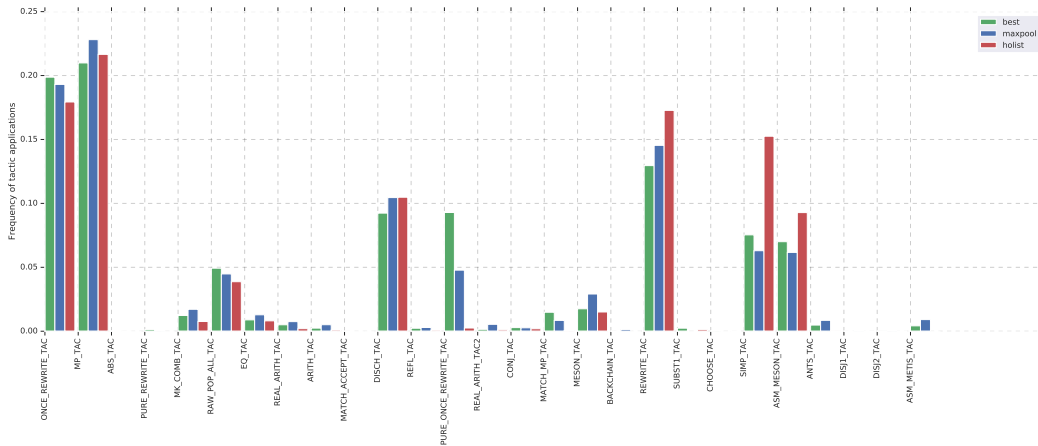


Figure 5: A comparison of the distribution of tactic application of our best model “best” versus “holist” versus the max pooling network “maxpool”. The height of the histogram indicates the relative frequency for a particular tactic among all successful tactic applications.